

Effect of Poly(Oxanorbonene)- and Poly(Methacrylate)-Based Polyzwitterionic Surface Coatings on Cell Adhesion and Gene Expression of Human Keratinocytes

Alice Eickenscheidt, Valentine Lavaux, Stefan Paschke, Alejandro Guajardo Martínez, Eric Schönemann, André Laschewsky, Karen Lienkamp,* and Ori Staszewski*

Polyzwitterions are generally known for their anti-adhesive properties, including resistance to protein and cell adhesion, and overall high bio-inertness. Yet there are a few polyzwitterions to which mammalian cells do adhere. To understand the structural features of this behavior, a panel of polyzwitterions with different functional groups and overall degrees of hydrophobicity is analyzed here, and their physical and biological properties are correlated to these structural differences. Cell adhesion is focused on, which is the basic requirement for cell viability, proliferation, and growth. With the here presented polyzwitterion panel, three different types of cell-surface interactions are observed: adhesion, slight attachment, and cell repellency. Using immunofluorescence methods, it is found that human keratinocytes (HaCaT) form focal adhesions on the cell-adhesive polyzwitterions, but not on the sample that has only slight cell attachment. Gene expression analysis indicates that HaCaT cells cultivated in the presence of a non-adhesive polyzwitterion have up-regulated inflammatory and apoptosis-related cell signaling pathways, while the gene expression of HaCaT cells grown on a cell-adhesive polyzwitterion does not differ from the gene expression of the growth control, and thus can be defined as fully cell-compatible.

1. Introduction

It is well known that surface properties, such as surface free energy, wettability, swellability, zeta potential, elastic modulus, and roughness have a major impact on the interaction of mammalian cells with biomaterials.^[1] In the case of polymer-based biomaterials, these surface properties are related to the chemical structure and surface architecture of the polymers used, including their charge per repeat unit, polymer chain hydrophobicity, chain mobility, molecular connectivity, degree of cross-linking, and surface topography. Thus, molecular features of the polymer can be used to control and direct the physical interactions of mammalian cells with biomaterials. For example, blood-compatible and cell-repellent surfaces have been designed from hydrophilic polymers like poly(ethylene glycol) or poly(acrylamide).^[2] Polymers functionalized with specific

A. Eickenscheidt, V. Lavaux, S. Paschke
Department of Microsystems Engineering (IMTEK)
University of Freiburg
Georges-Köhler-Allee 103, 79110 Freiburg, Germany

A. Eickenscheidt, V. Lavaux, S. Paschke
Freiburg Center for Interactive Materials and Bioinspired Technologies (FIT)
University of Freiburg
Georges-Köhler-Allee 105, 79110 Freiburg, Germany

A. G. Martínez, E. Schönemann, A. Laschewsky
Institut für Chemie
Universität Potsdam
Karl-Liebknecht Str. 25, 14476 Potsdam-Golm, Germany

A. Laschewsky
Fraunhofer Institut für Angewandte Polymerforschung
14476 Potsdam-Golm, Germany

K. Lienkamp
Department of Materials Science
Saarland University
Campus, 66123 Saarbrücken, Germany
E-mail: karen.lienkamp@uni-saarland.de

O. Staszewski
Institute for Neuropathology
Medical Center of the University of Freiburg
Hugstetter Str. 55, 79106 Freiburg, Germany
E-mail: ori.staszewski@uniklinik-freiburg.de

 The ORCID identification number(s) for the author(s) of this article can be found under <https://doi.org/10.1002/mabi.202200225>

© 2022 The Authors. Macromolecular Bioscience published by Wiley-VCH GmbH. This is an open access article under the terms of the Creative Commons Attribution-NonCommercial-NoDerivs License, which permits use and distribution in any medium, provided the original work is properly cited, the use is non-commercial and no modifications or adaptations are made.

DOI: 10.1002/mabi.202200225

biomolecules, on the other hand, enable selective cell attachment.^[3] For example, in the context of re-endothelialization of stents, it was shown that a drug-eluting stent coated with the biofunctional acrylate-based polymer BTL01015 enhanced the proliferation of human aortic endothelial cells, while the proliferation of coronary artery smooth muscle cells was suppressed.^[4] Adsorption of cells on surfaces is often mediated by proteins. Thus, it is clear that cell adhesion or repellency is often correlated to the adhesiveness or repellency of a material for proteins.^[5]

Polyzwitterions are polymers that contain the same amount of positive and negative charges per repeat unit and are thus overall charge neutral. In the context of biomedical applications, they are attracting an increasing interest due to their cell and protein-repellency, which prevents biofilm formation, combined with their cell compatibility and non-thrombogenic properties.^[6–10] In some cases, polyzwitterions that even become antimicrobial in the presence of bacteria have been reported.^[6,11–13] Polybetaines are a sub-class of polyzwitterions and contain a strong polycation (i.e., a cation that is pH-inert) combined with different anionic groups. Most polyzwitterions reported in the literature so far consist of positively charged quaternary ammonium ions, which are combined with phosphate, sulfonate, or carboxylate anions. Depending on the nature of the anionic groups, they are referred to as poly(phosphobetaines), poly(sulfobetaines), or poly(carboxybetaines), respectively.^[14–17] While some polyzwitterionic homopolymers have an upper critical solution temperature,^[18] the copolymers presented in this work do not show these properties in the range of investigation. Most polyzwitterions have been reported as cell-repellent,^[19,20] yet recent evidence shows that there are exceptions to this rule:^[6] in fact, a small number of surface-attached polyzwitterionic networks with carboxybetaine or sulfobetaine groups were shown to be both cell-adhesive and cell compatible.^[6,11–13] In these studies, the biological interaction of the cells with the specific polyzwitterions was studied by optical and fluorescence microscopy, and the Alamar Blue and MTT assays.^[6,11–13] While these methods are immensely helpful to investigate cell adhesiveness and toxicity of biomaterials, a deeper understanding of the underlying biological mechanisms that are triggered by the material-cell interactions cannot be obtained in this way. Indeed, detailed investigations including molecular biology methods have so far only been rarely reported in the context of polyzwitterions.^[21,22] On the other hand, even very detailed physical surface characterization data (surface morphology, surface zeta potential measurements, surface hydrophobicity, and local elastic moduli) only partially revealed the relevant parameters for keratinocyte adhesion or non-adhesion on polyzwitterions, and in fact, these results could not be used to fully predict the adhesiveness of keratinocytes on biomaterials.^[11] For the readers' convenience, the most important characterization data of the polyzwitterions A (called PSB in the original work)^[11] and B (called PCB in that same paper), which are studied in more detail in this paper, are summarized here: the static, advancing and receding contact angles were almost the same (A: 37°, 56°, and 22°; B: 36°, 55°, and 21°), indicating very similar surface energy for both materials. The swellability of A in pure water was 1.60, in 0.15 M NaCl it was 1.66 at pH 3 and 1.82 at pH 7. That of B was slightly higher: 1.9 in pure water, 1.76 at pH 3/0.15 M NaCl, and 1.94 at pH 7/0.15

M NaCl. The zetapotential of the pH-inert poly(sulfobetaines) A hardly changed in the pH range from 5 to 11. It had a zetapotential of –34 mV at physiological pH, which increased in acidic conditions to a maximum value of 0 mV, so that the isoelectric point was at pH 2.4. On the other hand, the zetapotential of the pH-responsive poly(carboxybetaine) B was positive in the acidic range (up to 50 mV); it had an isoelectric point at pH 5.4, and a negative zetapotential of –28 mV at physiological pH.^[11] Adsorption of several biological entities on these two materials was studied by surface plasmon resonance spectroscopy (SPR). In this context, reversible adsorption refers to biological matter that could be removed by rinsing with water, while irreversibly attached matter remained on the surface after washing. Adsorption of the model protein fibrinogen in the presence of bivalent Mg²⁺ cations resulted in no visible adsorption of any kind on poly(carboxybetaine) B, while some reversible but no irreversible interaction with poly(sulfobetaine) A was observed. Exposure to 100% human blood plasma led to some reversible adsorption on B, with only 0.47 ng mm⁻² plasma proteins adhering irreversibly. On poly(sulfobetaine) A, on the other hand, 6.3 ng mm⁻² plasma proteins remained irreversibly adhered. When exposed to human blood serum (100%), minimal reversible adsorption was observed, with hardly any irreversible adhesion (0.27 ng mm⁻² on A, 0 ng mm⁻² on B). These data are consistent with A being adhesive for mammalian cells, while cells could not adhere on B. Similar results were obtained when the materials were exposed to *Staphylococcus aureus* bacteria (10⁸ bacteria cm⁻³): no reversible or irreversible adhesion was found on B, while 1.8 ng mm⁻² remained irreversibly adhered on A. On the other hand, neither surface had a significant adhesion of *Escherichia coli* bacteria (A: 0 ng mm⁻², B: 0.02 ng mm⁻²).

One further particularity of thin layers of surface-attached polymer networks, which are the focus of the present study, is that some of their properties, for example, Young's modulus, are dominated by the properties of the underlying substrate, while other properties such as swellability are largely unaffected. This must be taken into account when studying these materials.

Successful initial adhesion of cells on surfaces depends on the ability of a single cell to adhere to another cell, to the extracellular matrix (ECM), or to a substrate.^[23] Cell adhesion is a complex process involving physical interactions, chemical binding events, and biological signaling processes. These regulate cell differentiation, the cell cycle, cell migration, and cell viability on surfaces.^[24] Contacts between the cell and the ECM occur via hemidesmosomes and focal adhesion points (FAs). In addition to the structural connection between the ECM and the actin cytoskeleton (through structural proteins such as talin and vinculin), which primarily influences cell movement, FAs are also important sites of signal transduction. Cellular processes such as proliferation and differentiation are additionally controlled by signaling molecules such as the focal adhesion kinase (FAK), the tyrosine kinase Src (acronym for sarcoma), and the protein paxillin.^[25–27] FAK is a non-receptor tyrosine kinase that is activated in the adhesion complex by binding to integrins. Activation occurs through autophosphorylation at tyrosine 397 (Tyr397, Y397), which is a binding site for the Src family kinases, and plays a key role in integrin-initiated signaling pathways.^[28,29] The phosphorylated form of FAK (pFAK) is therefore an excellent marker to detect stable adhesion of cells to a surface, and to distinguish

it from earlier stages of adhesion such as sedimentation or initial cell attachment.

To clarify the biological mechanisms that contribute to cell adhesion on polyzwitterionic surfaces, the aim of this study was to identify the biological pathways that contribute to the initial cell adhesion using a panel of structurally different polyzwitterions, and to correlate these biological responses with the chemical and physical properties of the materials. After a first screening of the cell adhesiveness of these polymers, immunofluorescence stains were used to detect FAKs on the selected polymers, and to analyze the cell morphology in more detail. To address the question of which genes are active when cells adhere to polyzwitterionic biomaterials (or not), a gene expression analysis was performed using Affimetrix microarrays. With this workflow, this work can also be considered as a blueprint for more detailed molecular biological studies, which may be useful when the routinely done physical-chemical and biological characterization methods established in the field do not sufficiently explain the materials' bioactivity profile.

2. Results

2.1. Design of the Study

As the aim of this study was to investigate the cellular events that lead to enhanced adhesion and viability of keratinocyte cells on surface-attached polyzwitterionic networks with different chemical structures and physical properties, first a panel of polyzwitterions with the desired structural characteristics was selected. As shown in **Figure 1**, these polymers differed in their overall hydrophobicity (contained either in the polymer backbone, or in the alkyl spacers of the polymer repeat unit side chains), and in the charged functional groups that form the zwitterionic repeat units (carboxylates, sulfonate, sulfate, ammonium, pyridinium). The polymers were first characterized with respect to their physical properties (e.g., by measuring their swellability and water contact angles). Local elastic moduli were not determined because these are dominated by the underlying substrate, and are all in the GPa range. Then, the keratinocyte viability and adhesion on the materials were investigated by microscopic methods, and by the using Alamar Blue cell viability assay. The polyzwitterionic materials were then classified according to the results of these studies. Expectedly, most surfaces were non-adhesive for keratinocytes (category 1). Other candidates were fully cell-adhesive (category 2). On one material, only small clusters of slightly adhering cells were found, that is, this material was barely adhesive for the keratinocytes (category 3). Selected members of categories 2 and 3 were then treated with immunofluorescence stains to image the FAs of the keratinocytes, and with fluorescence stains to visualize the actin filaments and the cell nucleus. This step was omitted for category 1 materials as it was clear that these would not contain FAs. Instead, to better understand the biological processes that were fundamentally different a category 1 and a category 2 polymer, differences in the gene expression and the related cell signaling pathways of representative materials were compared using Affimetrix microarrays, as described in detail below. Due to the high cost of the latter experiments, and because it was yet unclear whether this assay would reveal any differences at all, they

were only performed with the two borderline cases of one fully adhesive and one fully non-adhesive material.

2.2. Polymer Selection, Syntheses, and Surface Immobilization

2.2.1. Polymer Selection

The panel of polyzwitterions used in this study is shown in **Figure 1**. **Table 1** summarizes their structural characteristics and highlights their differences (backbone, charged groups, alkyl spacers in the side chain). Structures A and B (**Figure 1a,b**) are based on a poly(oxanorbornene)-backbone which is relatively hydrophilic and was obtained by ring-opening metathesis polymerization (ROMP).^[11,12] These two polymers are the only homopolymers in the study, and were cross-linked to form surface-attached polymer networks with an external tetrathiol cross-linker (**Figure 2a**).^[11,12] Polyzwitterion B is the only compound in the panel that contains carboxylates as anionic groups, while polyzwitterion subsets C, D, and E contain either sulfonates or sulfates. Polymer A is structurally similar to B but carries a sulfonate group. The other polyzwitterions were based on poly(methacrylate) backbones (C, D₁–D₄, E₁–E₄), or a poly(methacrylamide) (D₅) backbone and were synthesized by statistical free radical copolymerization. This allows the incorporation of 2-(4-benzoylphenoxy)-ethylmethacrylate (BPEMA) repeat units, where the 4-benzoylphenoxy ("benzophenone") groups act as photo-reactive cross-linkers, which transform the soluble copolymers into surface-attached polymer networks by UV-triggered C,H insertion reactions (**Figure 2b**).^[30,31] Structure C is unique in this panel since it is the only polymer that contains pyridinium as a cationic group (**Figure 1c**), while all the other polymers bear quaternary ammonium groups. Polymers D₁ and D₂ are made of the same zwitterionic monomer (containing sulfonate and ammonium groups, "sulfobetaine"), while their cross-linker content was varied (1% and 5%, respectively) to explore the effect of the cross-linking density on the bioactivity. Except for D₂, the cross-linker content was kept to 1% in all methacrylate-based polymers. Structure D₃ is the sulfate analog to D₁ which contains sulfonate groups. In D₄, the distribution of charges in the side chain is altered compared to all other D polymers, while in D₅, the overall hydrophobicity and flexibility of the side chains were modulated: the linkers connecting the backbone to the zwitterionic side chains of D₁ and D₅ differ by one CH₂ group, and the anchoring heteroatom was changed from oxygen (methacrylate) to nitrogen (methacrylamide) (**Figure 1d**). The terpolymers E₁ to E₃ (**Figure 1e**) differ in the contents of hydrophobic butyl methacrylate (BMA) units. Thus, they can be considered as structural analogs to D₁ with systematically increased hydrophobicity and reduced ion density. Like D₁, all are sulfobetaines containing quaternary ammonium and sulfonate groups. Analogously to the variation between D₃ and D₁, E₄ is the sulfate analog to E₁, but otherwise structurally identical. Overall, polyzwitterions bearing three different anionic groups and two different cationic groups were used. Most polymers contain the sulfonate group (A, C, D₁, D₂, D₄, D₅, E₁–E₃), two the sulfate group (D₃, E₄), and only B the carboxylate group. Except for C, all polymers have quaternary ammonium groups. Hence, a broad range of polyzwitterions with differences in hydrophilicity,

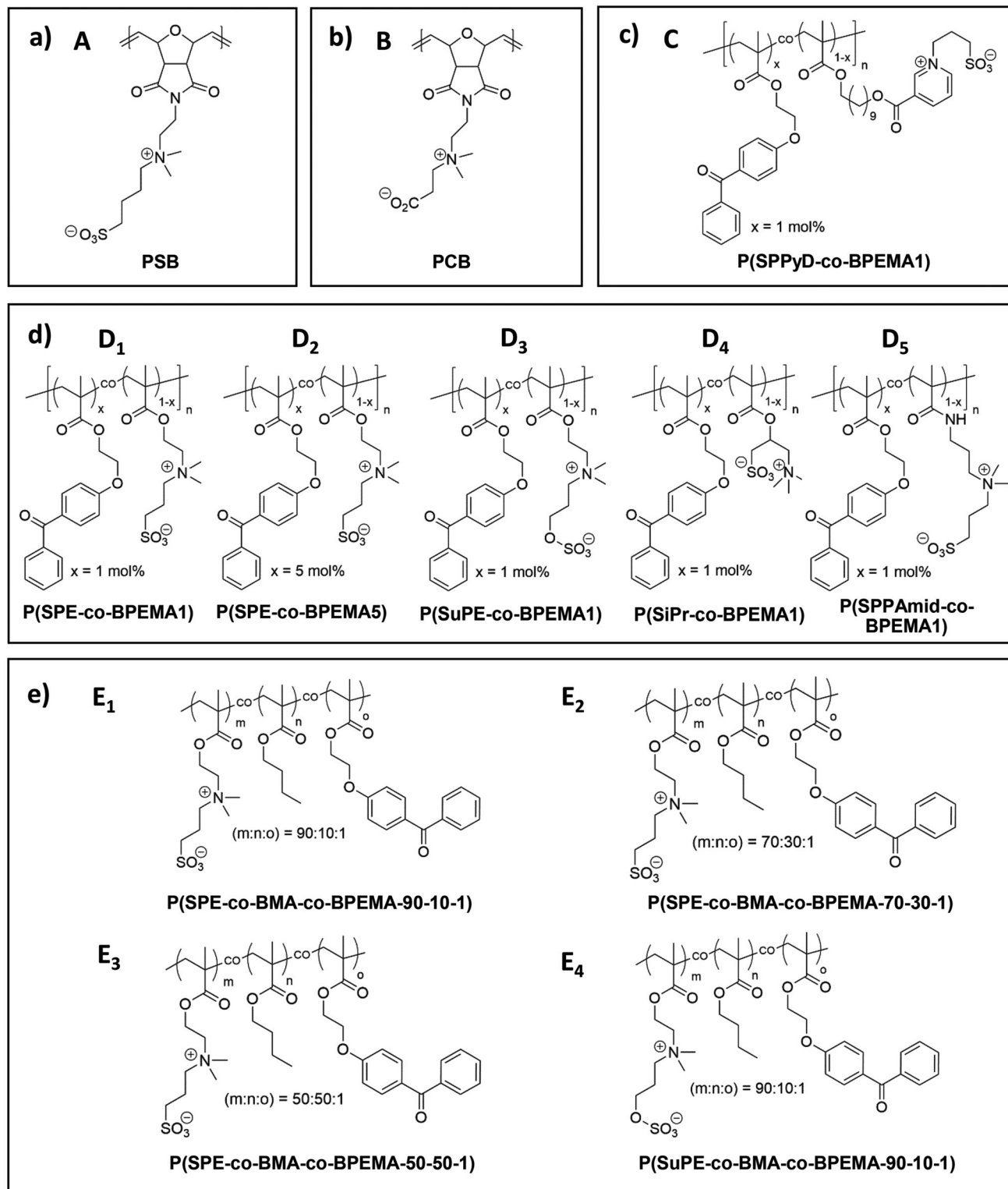


Figure 1. Sample-IDs, polymer names, and chemical formulae of polyzwitterions examined in this study. a) Poly(sulfobetaine) A (PSB), b) Poly(carboxybetaine) B (PCB), c) Statistical copolymer C with zwitterionic and UV-reactive 2-(4-benzoylphenoxy)-ethylmethacrylate (BPEMA) repeat units, d) Copolymers D₁ to D₆ with zwitterionic and UV-reactive BPEMA comonomers, e) Statistical terpolymers E₁ to D₄ with zwitterionic repeat units, BMA repeat units, and BPEMA repeat units

Table 1. Summary of the polyzwitterions used in this study, highlighting their backbone type, kind of charged groups, and spacer type.

Sample-ID	Name	Backbone	positively charged group	negatively charged group	R ¹	R ²	Ref.
A	PSB	Oxa-norbornene	R ¹ R ² N ⁺ Me ₂	Sulfonate	Ethyl	Butyl	[11]
B	PCB	Oxa-norbornene	R ¹ R ² N ⁺ Me ₂	Carboxy-late	Ethyl	Ethyl	[11]
C	P(SPPyD-co-BPEMA1)	Meth-acrylate	R ¹ O(C=O)py ⁺ R ²	Sulfonate	Decyl	Propyl	[30,32]
D ₁	P(SPE-co-BPEMA1)	Meth-acrylate	R ¹ R ² N ⁺ Me ₂	Sulfonate	Ethyl	Propyl	[30,32]
D ₂	P(SPE-co-BPEMAS)	Meth-acrylate	R ¹ R ² N ⁺ Me ₂	Sulfonate	Ethyl	Propyl	[33]
D ₃	P(SuPE-co-BPEMA1)	Meth-acrylate	R ¹ R ² N ⁺ Me ₂	Sulfate	Ethyl	Propyl	[30]
D ₄	P(SiPr-co-BPEMA1)	Meth-acrylate	R ¹ N ⁺ Me ₃	Sulfonate	1,3-Propyl	-	[30,32]
D ₅	P(SPPAmid-co-BPEMA1)	Methacryl-amide	R ¹ R ² N ⁺ Me ₂	Sulfonate	Propyl	Propyl	[30,32]
E ₁	P(SPE-co-BMA-co-BPEMA-90-10-1)	Meth-acrylate	R ¹ R ² N ⁺ Me ₂	Sulfonate	Ethyl	Propyl	[30,32]
E ₂	P(SPE-co-BMA-co-BPEMA-70-30-1)	Meth-acrylate	R ¹ R ² N ⁺ Me ₂	Sulfonate	Ethyl	Propyl	[30,32]
E ₃	P(SPE-co-BMA-co-BPEMA-50-50-1)	Meth-acrylate	R ¹ R ² N ⁺ Me ₂	Sulfonate	Ethyl	Propyl	[30,32]
E ₄	P(SuPE-co-BMA-co-BPEMA-90-10-1)	Meth-acrylate	R ¹ R ² N ⁺ Me ₂	Sulfate	Ethyl	Propyl	[30,32]

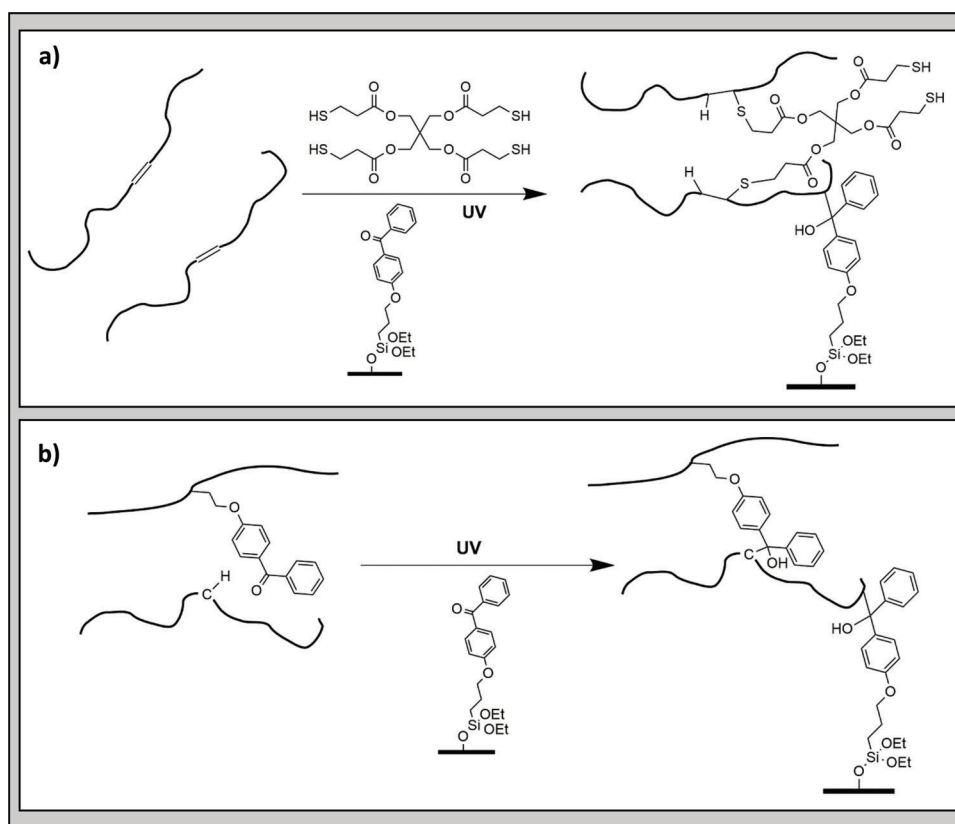


Figure 2. Crosslinking of zwitterionic polymers by different mechanisms. a) UV-activated thiol-ene reaction between an external tetrathiol crosslinker and double bonds in the polymer main chain; b) UV-activated C,H insertion reaction using an internal, covalently attached benzophenone cross-linker.

chemical hardness of the charges involved, and dipole orientation was investigated.

2.2.2. Synthesis

The synthesis procedures of the polymers investigated were reported before: A and B were synthesized via ring-opening

metathesis polymerization (ROMP).^[11,12] All other polymers were prepared via free radical polymerization (FRP). The synthesis was described in detail for polymers D₁ and D₅ in ref. [32], for D₂ in ref. [33], for D₃ in ref. [30], for D₄ in ref. [34], and for E₁ to E₃ in ref. [35]. Polymers C and E₄ were prepared analogously to D₁ and E₁, employing the respective zwitterionic methacrylates that were described before.^[36]

Table 2. Physical and biological characterization of surface-attached polyzwitterion networks. Ellipsometry was used to determine the layer thickness, and atomic force microscopy (AFM) was used to measure the roughness. The static, advancing, and receding CAs were measured. Swellability was determined using SPR. For A and B, literature data was used. Cell adhesion was studied by microscopy methods as discussed below.

Polymer	Thickness [nm]	CA [°] static, adv., rec.	Roughness [nm]	Swellability	Cell Adhesion
A ^[11]	71 ± 3	37 ± 2 56 ± 2 22 ± 2	19	1.6	adhesion and elongation
B ^[11]	89 ± 3	36 ± 2 55 ± 2 21 ± 2	17	1.9	None
C	216 ± 3	71 ± 2 73 ± 2 14 ± 4	16	n.d.	adhesion and elongation
D ₁	176 ± 3	54 ± 6 55 ± 4 23 ± 4	0.4	2.4	None
D ₂	177 ± 6	70 ± 3 62 ± 2 25 ± 2	4.3	n.d.	None
D ₃	108 ± 6	63 ± 2 61 ± 2 27 ± 5	7.2	2.1	None
D ₄	154 ± 4	56 ± 7 55 ± 8 18 ± 1	0.3	n.d.	None
D ₅	125 ± 4	63 ± 6 60 ± 7 27 ± 4	0.3	n.d.	None
E ₁	113 ± 4	77 ± 3 75 ± 2 27 ± 3	0.3	3.1	None
E ₂	161 ± 4	85 ± 3 87 ± 2 27 ± 2	1	3.0	None
E ₃	152 ± 2	75 ± 1 77 ± 1 21 ± 5	7.1	n.d.	None
E ₄	220 ± 5	55 ± 2 56 ± 1 22 ± 3	1.4	n.d.	slight attachment, no elongation

2.2.3. Surface Immobilization

To obtain surface-attached polymer networks, silicon wafers (for ellipsometry and water contact angle measurements), glass coverslips (for cell culture), or gold substrates (for SPR measurements) were used as substrates. These were functionalized with linker molecules (Figure 2) as described in the literature.^[11] For A and B, networks were synthesized using pentaerythritol-tetrakis(3-mercaptopropionate) as an external cross-linker (Figure 2a). A solution of both components was spin-cast onto the substrate and cross-linked by irradiation with UV-light.^[11] The surfaces were then washed with trifluoroethanol (TFE) to remove loose polymer chains. All other polymers contained between 1 and 5 mol% of repeat units carrying the internal UV-cross linker benzophenone (BPEMA). They were also spin-coated onto the respective substrates from solution, directly cross-linked by UV-irradiation, and washed with TFE to remove poly-

mer chains that were not part of the surface-attached network (Figure 2b).

2.3. Physical Characterization and Protein Adhesion Studies

As it is well-known that the cell compatibility of polymer surfaces is related to their surface chemistry and physical properties,^[1] several important properties of the polyzwitterions listed in Table 1 were studied. The results (layer thickness, determined by ellipsometry), surface roughness (studied by atomic force microscopy, AFM), and swellability (determined by SPR) are summarized in Table 2. The local elastic moduli were not determined for the above-mentioned reasons. The data for A and B were reported previously.^[11] Except for A and B, the thickness of all networks was higher than 100 nm. Based on previous experience with this type of coating, this thickness is sufficient for

complete surface coverage, and thus assures that the data acquired in the following biological experiments is related to structural differences of the surface coatings, and not to coating defects. The static and dynamic water contact-angles (CAs) of the surfaces were measured to estimate their hydrophilicity, and are also included in Table 2. The receding contact angles agreed well with the values previously reported. However, the static contact angle data are in several cases significantly higher than the previously reported data.^[11,12,32,33] This could be explained by differences in the measurement routine, the sample storage time, or the sample storage conditions. As these surface-attached polymer networks have a low cross-linking density, and hence significant structural flexibility, the contact angle differences between the determined data set and the literature data could be due to molecular rearrangements at the interface, particularly of the hydrophobic moieties of the polymers, that occur to lower the overall surface energy of the system when stored in air. Interestingly, for the series E₁ to E₃, one previous study also found that E₂ had the highest static contact angle of the three,^[35] although it was not the polymer with the highest fraction of hydrophobic butyl repeat units. While the reasons for these results are not yet understood (and indeed are not the main focus of this work), this qualitative agreement in the data conforms to the validity and consistency of the here presented measurements.

The surface morphology and roughness of each sample were studied by AFM (Figure S1, Supporting Information). Polyzwitterions A and B showed a high surface roughness due to the external cross-linker used to form surface-attached networks. A microphase separation of the polymer and the external cross-linker upon film formation has been reported previously, but does not negatively affect the overall macroscopic surface properties.^[11] Surfaces made from D₃ showed a slightly increased surface roughness compared to the other poly(methacrylate)-based surfaces. This polymer was also the one with the lowest solubility in TFE. The roughness also increased with the increasing BPEMA-content in D₁ and D₂ as well as with the increasing BMA-content from E₁ to E₃.

Measuring the swellability by SPR is a quite elaborate experiment; therefore it was only performed for selected samples. Swellability depends on two factors: hydrophilicity and cross-linking density. Assuming that the cross-linking density was comparable for A and B, the poly(sulfobetaine) A was less swellable in water than the poly(carboxybetaine) B. Since A and B were cross-linked differently than all the other polymers, these values cannot be used to compare the relative hydrophilicity of these two polymers with the rest of the sample set. Out of the sample set with the internal benzophenone cross-linker, the poly(sulfobetaine) D₁ had a slightly higher swellability than the poly(sulfobetaine) D₃. The same trend was observed in the contact angle measurements. The swellability of the polymers E₁ and E₂ (with 10% and 30% BMA repeat units, respectively) was about the same (3.0 and 3.1), but unexpectedly higher than that of polymers D₁ and D₃ (2.1 and 2.3) without additional hydrophobic BMA groups. As this observation did not match the contact angle data (where the values for E₁ and E₂ were larger than for D₁ and D₃, as would be expected based on chemical intuition), it is possible that the state of cross-linking was different for the D and the E polymers. One could speculate that some kind of molecular rearrangement of the dry film takes place in the E polymers

prior to UV cross-linking (e.g., clustering of the butyl residues to avoid contact with the charged repeat units), which makes these groups less available for UV cross-linking and thus gives films which swell more strongly. That some kind of structure formation is happening in these films can be seen from the roughness increase in the AFM measurements.

2.4. Biological Characterization

2.4.1. Choice of the Cell Line, Biological Assays, and Validation Controls

Keratinocytes from a spontaneously immortalized human keratinocyte cell line (so called HaCaT cells)^[37] were used to test the cell compatibility of the surface-attached polyzwitterion networks, to distinguish between cell-adhesive and cell-repellent polymers, and to investigate the biological processes occurring during cell-surface interaction. In vitro, this cell line exhibits all the functional activity and major surface markers that are characteristic for keratinocytes isolated from healthy tissue.^[11,37] HaCaT cells are thus a suitable model system for our purpose. The HaCaT cells were cultivated using standard procedures as described in the Experimental. They were then plated out onto polyzwitterion-coated glass coverslips. Uncoated glass coverslips were used as reference samples, together with fibronectin-coated coverslips as an additional reference. This additional reference was chosen because cells usually interact with specific cell binding sites of the ECM (e.g., glycoproteins like collagen, fibronectin, and laminin) via integrins. Materials coated with these proteins are therefore often used as additional references in cell culture assay to better mimic the cellular growth under natural conditions, or simply to improve substrate adhesion.^[38–41] Optical microscopy was used as a screening tool to sort the polyzwitterionic coatings into the three categories mentioned above according to their cell adhesiveness. All samples were studied using the Alamar Blue assay to monitor the metabolic activity of HaCaT cells grown on them, which is an indicator of cell viability.^[11,12] The results of the Alamar Blue assay were subsequently confirmed with a live-dead stain which detects cell damage.^[11,12] Once the polyzwitterions were categorized, polymers from categories 2 and 3 were selected for further biological characterization. These were: polymer E₄ on which cells only slightly attached (category 3), and polymers A and C, on which cells firmly adhered (category 2). They were further stained with (immuno)fluorescence stains for the FAK, the cell cytoskeleton, and the nucleus, in order to detect the FA points and image the cell morphology in more detail. To study the gene expression of HaCaT cells that were cultivated in the presence of the cell-adhesive polyzwitterion A and the cell-repellent polyzwitterion B, the RNA of these cells was isolated. This RNA was then analyzed with Affimetrix microarrays to map the gene expression, and thereby detect potential differences in the activated cell signaling pathways of cells in contact with either polyzwitterion A or B.

2.4.2. Optical Microscopy, Alamar Blue Assay, and Live-Dead Stain

Figure 3 shows the results of the Alamar Blue assay and the optical microscopy images for selected polymers. Additional results

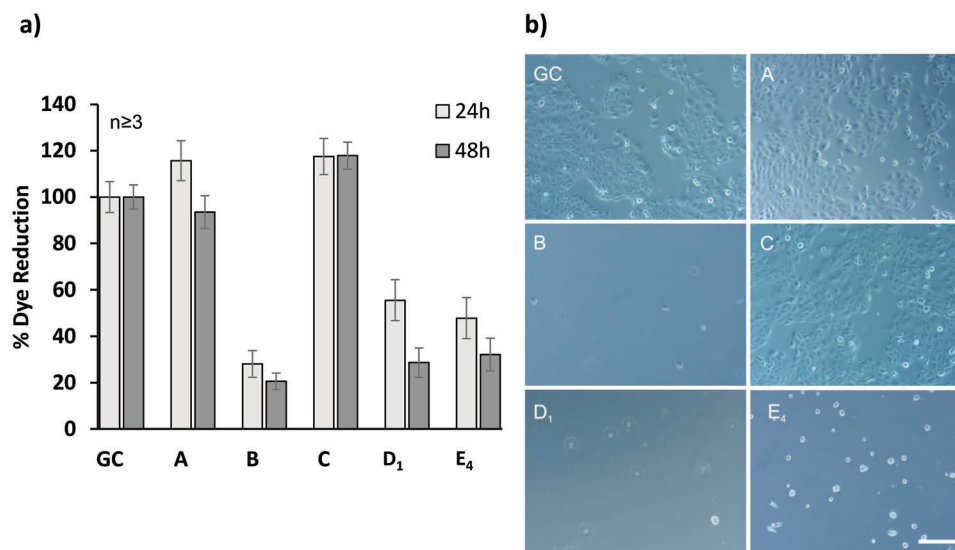


Figure 3. Cell compatibility of keratinocytes (HaCaT) on different polyzwitterions at 24 and 48 h after seeding. GC = growth control (uncoated glass coverslips), A, B, C, D₁, and E₄ = polymers with structures as indicated in Figure 1 and described above. a) Relative reduction of the Alamar Blue dye (normalized to the GC) by HaCaT cultivated on polyzwitterions. b) Representative optical microscopy images of the cell growth of HaCaT after 48 h. Scale bar: 200 μ m.

can be found in Figure S2, Supporting Information. In the Alamar Blue assay (Figure 3a), the relative dye reduction percentage, that is the reduction of the non-fluorescent dye resazurin to the fluorescent resorufin dye, normalized to the growth control (GC) (cells grown on the uncoated well bottom) is determined. The reduction of dye is proportional to the overall cell metabolism and thus depends on both the average level of metabolism in each individual cell, and on the total cell number. The data was recorded after 24 h and 48 h of cell growth in the presence of the respective surfaces. The growth of the cells after 48 h was also analyzed by optical microscopy to visualize the growing cell population (Figure 3b). Care must be taken not to over-interpret the optical micrographs. While the Alamar Blue assay gives quantitative information in a large analytical volume regarding the metabolic activity, the micrographs only qualitatively and locally represent the cell situation. The purpose of these images is to image the cell morphology (elongated cells adhere to the substrate, round cells do not adhere, cell clusters hint at the ability of cells to adhere to each other but not (well) to the surface). Also, by differentiating between “few” and “many” cells present, they help decide whether there is little dye reduction because there are no cells present, or because the cells present do not metabolize (a sign of cell toxicity). For example, hydrophobic, polycationic coatings can show a large number of adhering cells on the surface, but low dye reduction. A similarly low dye reduction can also be obtained if there are only a few cells present on a non-adhesive, non-toxic polyzwitterionic surface, which do metabolize but cannot adhere.

As expected, and as shown in previous studies,^[11] the cells grown on polyzwitterion A had a level of metabolic activity that was comparable to both the cells on the GC (Figure 3) and the additional fibronectin-coated coverslips (FN, Figure S3, Supporting Information). The cell number on A and on these controls was comparable, and the cells on A were elongated. On the other hand, polyzwitterions B and D₁ were proven to be cell-repellent, which can be seen in the lower dye reduction, as well as in opti-

cal microscopy images (Figure 3b), where only a small number of round, unattached cells could be observed. On the other hand, the metabolic activity of the cells grown on polyzwitterion C even surpassed the GC, indicating excellent adhesion and viability and a high cell number. Except for E₄, where only a small number of cells seemed to attach at the surface, all other polyzwitterionic surfaces listed in Figure 1 were cell-repellent (Figure S2, Supporting Information), which is in line with literature reports for most of the polyzwitterionic surfaces investigated so far.^[6] Based on these results, it is clear that polymers A and C fall into category 2, E₄ is the only representative of category 3, and all other polymers are category 1. Because of the physical similarity of the surfaces that fall into category 1, no further correlation between their chemical structure (effect of cross-linking density, content of BMA, and nature of the anionic group) and their biological properties can be derived.

The viability of the HaCaT cells on the thus analyzed polyzwitterions was further confirmed with a live-dead stain (Figure 4, showing the viability of cells in the GC, in the dead cell control (DC, cells treated for 10 min with 0.1% Triton X 100), of cells grown on FN-coated substrates, and of cells grown on substrates coated with polyzwitterion networks A, B, C, D₁ and E₄, respectively, after 48 h). The live-dead staining shows that the HaCaT cells on both A and C have the same level of vitality as those grown on GC and FN. Interestingly, the cells on E₄ are also vital, even though they seem to be unable to proliferate. In comparison to the GC, it seems as if they were able to attach to the surface, but not able to grow and form monolayers. Instead, they form clusters with each other, and their nuclei start to shrink. In contrast, polymers B and D₁ are strongly cell repellent, therefore only a few non-adhering, round cells are seen in these images.

Thus, it was demonstrated that all the polyzwitterions used did not have any direct toxic effects on the cells, as indicated by the live-dead stain. However, as indicated by the metabolic activity of the HaCaT cells, and by confirming the cell vitality

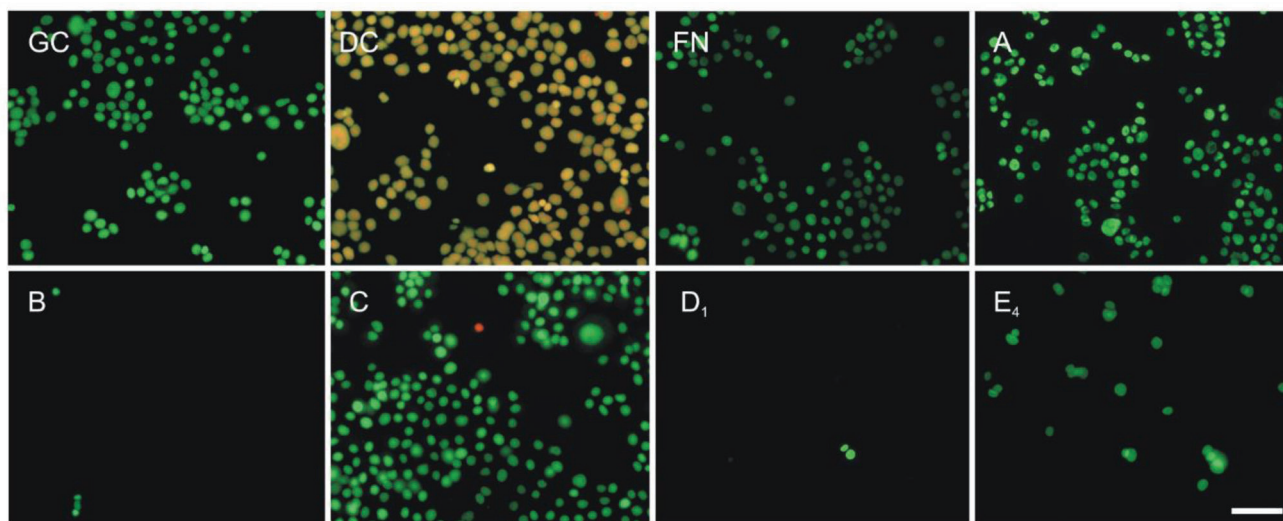


Figure 4. Live-dead staining of HaCaT after 48 h growth on polymers A, B, C, D₁, and E₄. Controls: GC (GC on glass coverslips), DC (dead control), and FN (fibronectin). Merge pictures of vital (Syto 16, green) and dead cells (Propidiumiodide, red). Except for the DC, cells are vital in all cases, but the cell number varies significantly: hardly any cells were found on B and D₁, while the cells proliferated well on A and C (monolayer formation). E₄ shows no monolayer but cell clumps of vital cells. Scale bar: 100 μ m

using the live-dead stain, marked differences with respect to cell adhesion were observed. The two polyzwitterions A and C were cell-adhesive, B and D₁ were cell-repellent, and E₄ was in between these two extremes. These results thus confirm the above-presented polymer classification based on the optical microscopy results.

2.4.3. Immunofluorescence Staining

The next step was to investigate to what extent the cell adhesion on the polyzwitterions differed between the materials and the controls, especially for E₄, on which cells were not able to adhere properly. To that end, the cellular expression of FAK was investigated using immunofluorescence methods. It is known that FAK is highly phosphophorylated in adhering cells.^[28] Therefore, we chose the FAK autophosphorylated at the tyrosine binding site Tyr397 (pFAK) as a marker for activated FAK. The results for HaCaT cells cultured on the controls GC, FN, and on Polymers A, C, and E₄ are shown in **Figure 5**. Column 1 of Figure 5 shows the cell nuclei that were stained blue with the 4',6-diamidino-2-phenylindole (DAPI) stain, column 2 displays the pFAK distribution of the cells (green), and column 3 the red actin stain, which was used to better visualize the edges of the cells and to analyze the shape of their cytoskeleton. The merged images and insets in Figure 5 (labeled "''") show a clear difference in the expression pattern of pFAK. Except for the cells grown on sample E₄, all cells show adhesion plaques in the periphery (small green dots at the edge of the cells), which in addition to the continuous cytosolic expression is a clear indication of FA.^[42,43] The data indicates that the cells grown on the polyzwitterionic networks A and C and on the controls have a comparable number and size of FAs. In contrast, no such expression pattern (no dots in the periphery) can be seen in cells grown on E₄. The cytoskeleton of the cells grown on E₄ is not elongated, therefore only cell clumps are seen, and it is

not possible to detect any of these peripheral expression patterns of pFAK that are necessary to confirm FA.

The absence of FAs could be the reason why the cells cultivated on these substrates could only loosely attach and were not able to elongate. Consequently, these cells were not able to form the 'cobblestone' pattern of confluent cells, which is typical for keratinocytes and necessary for cell vitality. Fluorescence staining was not applied to samples B and D₁, as it was clearly visible in the live dead-stain images that no cells attached to these surfaces. The outcomes of the cell adhesion experiments are summarized in the last column of Table 2.

From a chemical perspective and based on the results of the physical characterization, it is not clearly understood why the polyzwitterionic E₄ networks have this unexpected profile. The main structural difference of E₄ in comparison to the E₁ networks is the presence of the sulfate group instead of the sulfonate group in the zwitterionic moiety. Generally, the hydrophilicity of zwitterionic moieties containing the ammonium group as a common cation combined with varying anionic groups is considered to decrease from carboxylate to sulfonate to sulfate.^[44,45] This should render the network E₄ less hydrophilic and thus less cell-repulsive than E₁ (in analogy to the effect observed when comparing the contact angles of the polyzwitterionic networks D₁ and D₃). Indeed, E₄ was more cell-adhesive than E₁, yet no such increase in cell-adhesiveness was found for networks D₁ and D₃, indicating that the nature of the anionic group is not the sole contribution to this effect. Thus, further detailed studies are needed to explain this unprecedented behavior.

2.4.4. Gene Expression of HaCaT Cells Cultivated in the Presence of Polyzwitterion Networks A and B

In order to better understand the cellular behavior of HaCaT cells on adhesive and non-adhesive polyzwitterionic networks, their

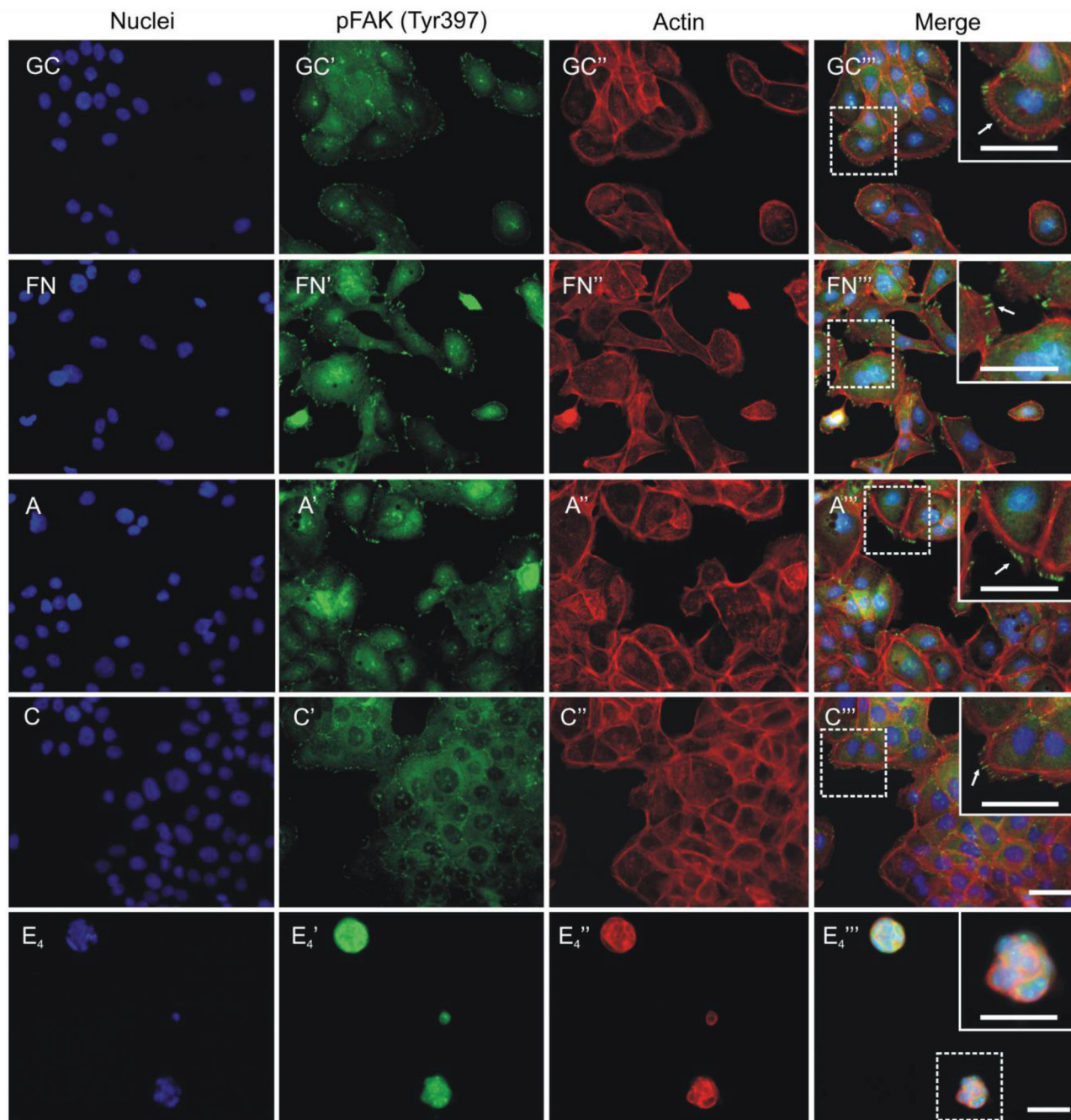


Figure 5. FA and cell morphology of HaCaT cells cultivated on surface-attached polyzwitterion networks after 48 h. Representative immunofluorescence micrographs of paraformaldehyde-fixed cells grown on uncoated substrates (GC-GC^{'''}), substrates coated with 10 $\mu\text{g mL}^{-1}$ fibronectin (FN-FN^{'''}), and glass coverslips coated with the three polyzwitterions A, C, and E₄ (A-A^{'''}, C-C^{'''}, and E₄-E₄^{'''}, respectively). Fluorescence was recorded on three channels to visualize the nuclear staining (DAPI, blue, first column, images A, C, and E₄), the antibody detection of phosphorylated FAK at Tyr397 (pFAK, green, alexa fluor 488, second column, A', C', and E₄'), and the actin cytoskeleton (red, phalloidin, third column, A'', C'', and E₄''). All channels were merged in the last column (A''', C''', and E₄'''). The insets in the last column show the formation of FAs on all surfaces except E₄'''. The expression of pFAK on the polyzwitterions A and C is comparable to the controls (GC, FN). These finger-like structures are highlighted by the arrows in the insets. There is no FA seen on E₄ networks. Instead, a compact cytoskeleton in HaCaT cell aggregates is seen. Scale bars: 50 μm .

gene expression after 24 h of cultivation on the polyzwitterionic networks A and B was analyzed using microarray experiments. Microarrays are frequently used in molecular biology to analyze changes in gene expression levels of cells due to different physical or chemical environments. In the microarray experiments used, first the messenger RNA (mRNA) produced by the cells after 24 h cultivation in contact with the test samples was isolated. The complementary DNA (cDNA) was then synthesized and amplified by the addition of oligonucleotide primers, resulting in complementary RNA (cRNA), which was labeled with biotin and fragmented. In a final step, the cRNA sample was hybridized with the markers on the microarray probe. Matching strand pairs were stained, so that the gene expression pattern could be determined by measuring the local distribution of the fluorescence intensity on the microarray.^[46] In light of the costliness of these experiments, and to determine whether such effects can be seen at all in the cellular gene expression, these analytics were performed for the two border cases only: the adhesive polyzwitterion A, and the non-adhesive polyzwitterions B.

Thus, gene expression of cells that were grown on the surface A and the GC was compared to cells that were cultivated in contact with surface B, but did not attach. These experiments were designed to analyze the cell signaling processes found in non-adhering cells while they are still viable. This should reveal whether the cells come into contact with the surface at all, and why their adhesion fails. The results of these experiments are presented as so-called volcano plots in **Figure 6**. In these plots, the differential expression of genes of HaCaT cell grown in the presence of either surface A or B after 24h are compared to the GC (Figure 6a,b), and to each other (Figure 6c), together with the intensity factor of these differences. Specifically, the statistical significance ($-\log_{10} p$ value, y axis) is plotted versus the magnitude of change in the gene expression (fold change, x axis). Genes that were the most up-regulated are shown on the right-hand side of the diagrams (red color), the ones that were the most down-regulated are displayed on the left-hand side (blue color). In between, the ones that showed no significant relevance are colored in grey. The comparison of the gene expression of B with the GC (Figure 6a) indicates a large number of significant differences in the gene expression (>1000 points). In particular, a large number of protein-encoding genes that are involved in the cell-cycle control are down-regulated. For example, DTL, the Denticleless E3 Ubiquitin Protein Ligase Homolog, which is a key regulator of genome stability and cell cycle progression,^[47] is significantly downregulated. On the other hand, genes that are involved in the initiation of apoptosis, the programmed cell death, for example, TNFSF10 (the Tumor Necrosis Superfamily Member 10, also known as TNF-related apoptosis-inducing ligand, TRAIL)^[48] are significantly up-regulated. The top 10 significant differences between surface B and the GC are labeled with the abbreviation of the related genes in Figure 6a. The full names corresponding to these abbreviations can be found in Table S2, Supporting Information. In Figure 6b, the gene expression of HaCaT cells cultivated on surface A compared to the GC is presented. This data indicates that there are hardly any significant changes between these two sample types, except for one gene that encodes a member of the serine proteinase inhibitor (serpin) superfamily (SERPINE1, Serpin Family E Member 1) which is down-regulated significantly. This gene functions as an inhibitor of fibrinolysis and

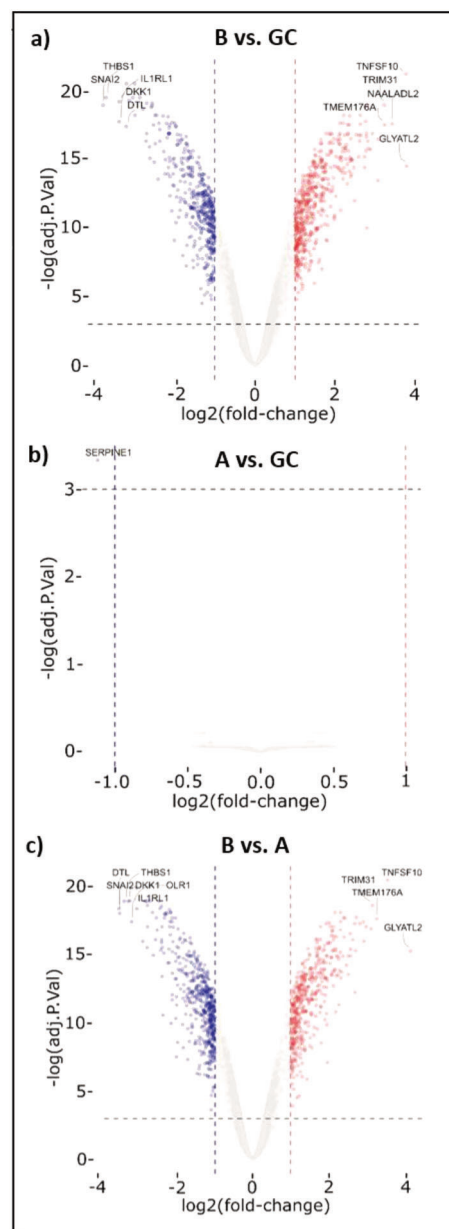


Figure 6. Differences in gene expression of HaCaT cells cultivated in the presence of polyzwitterion networks. a) Volcano plot for B vs. GC, with more than 1000 significant differences, b) A vs. GC, showing only one significant difference in the gene expression and c) B vs. A. Non-significant differences: grey; p value <0.05 : blue; absolute log fold change > 1 and p value <0.05 : red. The top ten most up- or down-regulated genes are highlighted in each Figure. Full gene names are given in Table S2, Supporting Information.

as a component of innate antiviral immunity. Thus, the gene expression study confirms that the growth of keratinocytes is completely unaffected by the presence of polyzwitterion A: the cells are viable and proliferate. With this data, we can provide evidence that these polyzwitterions are fully cell-compatible.

Due to the few differences observed between A and the GC, it is also instructive to analyze a volcano plot that directly compares

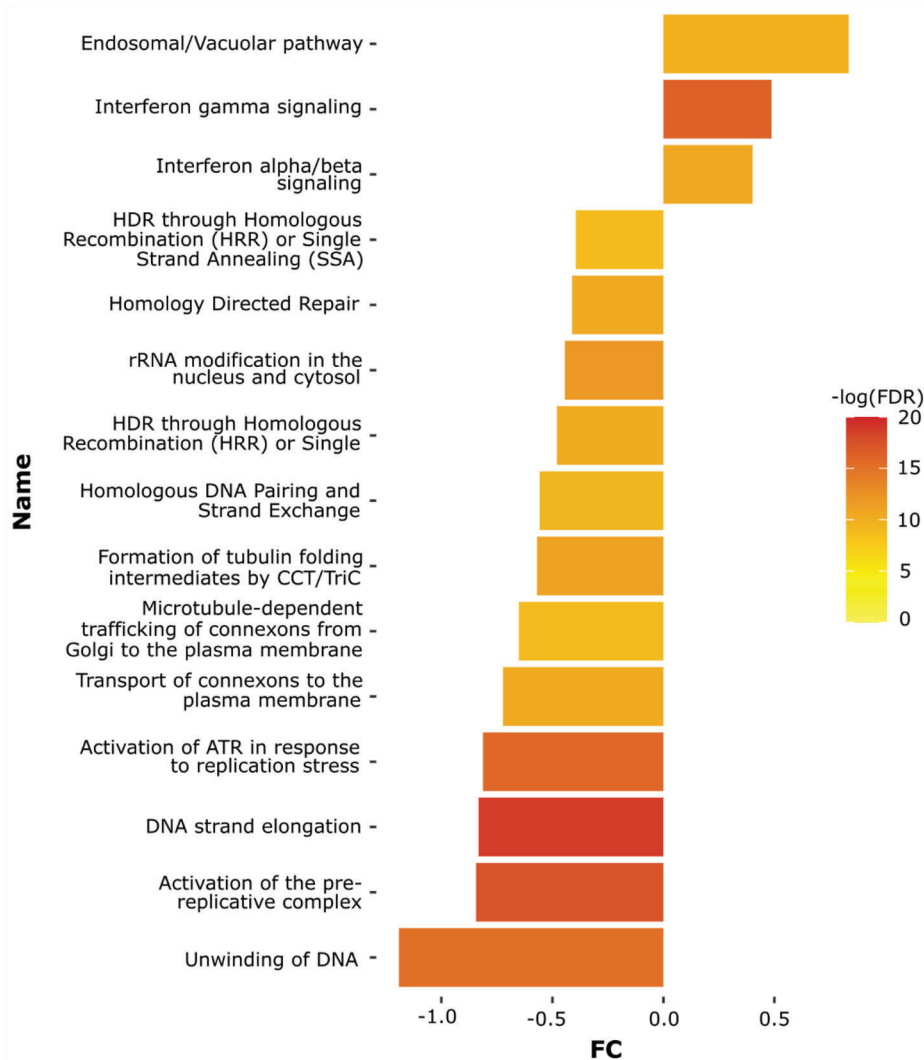


Figure 7. Analysis of gene expression changes in cells grown on polyzwitterion B, compared to the GC, using the Reactome Database. The fold change of activity (FC) of the respective pathway in comparison to $-\log_{10}(\text{FDR})$ (false discovery rate) is shown.

the gene expression of cells grown on polyzwitterions A and B. As shown in Figure 6c, the results are similar to those presented in Figure 6a, with a few exceptions: Besides the most strongly down-regulated genes THBS1, SNAI2, IL1RL1, DKK1, and DTL that were already highlighted in Figure 6a, OLR 1 appears as additional significant difference when comparing the surfaces of B and A (Figure 6c). On the other hand, when comparing the most strongly up-regulated genes, NAALADL2 appears among the top 10 significant genes in Figure 6a, but not in Figure 6c. The other most significantly up-regulated genes found in both figures are TNFSF10, TRIM31, TMEM176A, and GLYATL2.

To illustrate which function the genes labeled in Figure 6 have, and to better understand which signaling pathways are affected by the altered gene expression profile, we performed two further data analyses for the direct comparison of cells that were incubated on B vs GC. Using the Reactome Database,^[49] the observed gene expression changes were correlated with different cellular events (Figure 7). The factors by which these were up- and down-

regulated in B relative to the GC are shown as fold change of activity of genes, compared to $-\log_{10} \text{FDR}$ (false discovery rate). This analysis revealed an increase in interferon-regulated inflammatory signaling pathways, while pathways related to homeostatic DNA maintenance appear reduced in activity. A second analysis of the same data was performed using the Kyoto Encyclopedia of Genes and Genomes (KEGG) database.^[50,51] This analysis corroborates an increase in interferon signaling, and additionally suggests an up-regulation of senescence and apoptosis-related genes (Figure 8). Taken together, the data suggest an inflammatory response mediated through interferon signaling in cells incubated in the presence of surfaces coated with polyzwitterion B. Furthermore, these cells exit the normal growth phase, and either enter senescence or apoptosis, both of which are common endpoints for cells that accumulate damage or damage signals that render them incapable of homeostatic growth (Figure 8).

Thus, while the gene expression studies confirmed that the growth of keratinocytes on polyzwitterion A is unaffected by that

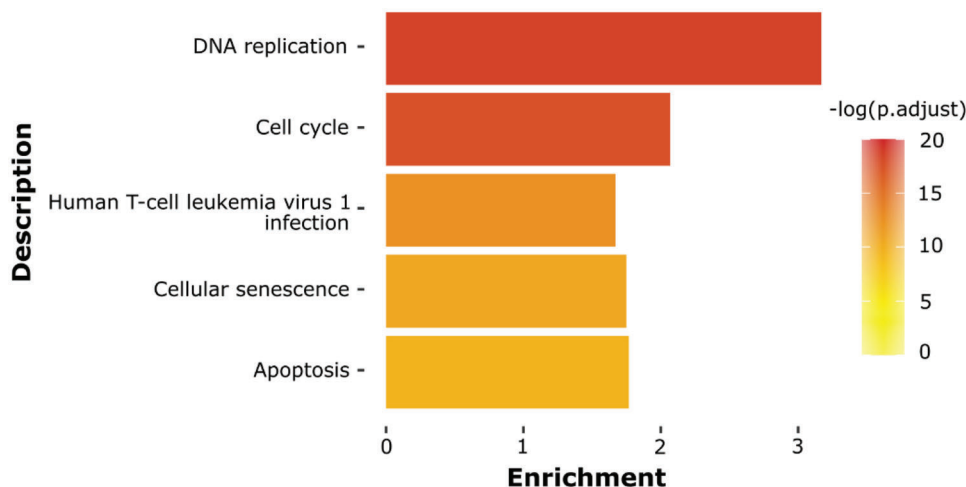


Figure 8. Analysis of increased cellular pathway activity in HaCaT cells grown on polyzwitterion B, compared to the GC, analyzed using the KEGG database. The y axis contains the pathway description, while the x axis indicates the enrichment factor. The color indicates the $-\log(p.adjust)$ value, that is, the statistical significance of the result.

polyzwitterion and comparable to the GC, the interaction of the cells with polyzwitterion B is quite different. Even though the keratinocytes were not able to bind to this surface, the gene expression analysis data implies that some kind of brief contact between the cells and the substrate must have taken place, as more than 1000 genes were dysregulated. The finding that cellular senescence and apoptosis pathways were increased in HaCaT cells incubated on B is plausible, since the cells were not able to attach and thus had to remain in suspension. However, cell adhesion is essential for healthy cell growth and proliferation, and if this is impossible the cells must eventually go into apoptosis. In addition, a dysregulation of cell cycle-associated pathways was detected using the KEGG database. However, as has been reported in the literature,^[52] apoptosis and cell cycle regulation have several common genes, therefore it is difficult to quantitatively distinguish between the two events with this method. Interestingly, interferon (IFN)-signaling associated pathways (IFN- α , IFN- β , and IFN- γ) that are highly associated with inflammation (reviewed in ref. [53]) are significantly up-regulated in cells grown in the presence of polyzwitterion B. It was previously described that poly(carboxyzwitterions) can induce the expression of cytokines in mice in vitro and in vivo.^[21] In this study, two sets of nanoparticles, one coated with poly(ethylene glycol) (PEG) and the other coated with a poly(carboxybetaine) were analyzed, and that poly(carboxybetaine) showed a potential immunotoxicity due to enhanced cytokine secretion compared to PEG. These data strengthen the result of our gene expression study and make it plausible that there is also an inflammatory effect of polyzwitterion B on mammalian cells. In another study, it was reported that hydrophilic nanogels made from a poly(carboxybetaine), a poly(sulfobetaine), and PEG could modulate the immune response of blood cells exposed to lipopolysaccharide, where the poly(carboxybetaine) had the strongest effect in alleviating the pre-existing immune responses in vivo, followed by the poly(sulfobetaine) and PEG.^[22] This trend was explained by the relative protein repellency and state of hydration of these three materials, which was strongest for the poly(carboxybetaine)s. This matches the results of this study in

so far as cells could adhere to the poly(sulfobetaine) A investigated here, but not to the potentially also more strongly hydrated poly(carboxybetaine) B. On the other hand, the cells that were in contact with poly(carboxybetaine) B suffered an inflammatory reaction, and finally went into apoptosis. The differences may be due to the difference in the cell lines used: the blood cells do not require a substrate to proliferate, and thus would not suffer from their inability to adhere to the poly(carboxybetaine).

Another set of pattern-recognition genes, the toll-like receptors (TLR) were also up-regulated on poly(carboxybetaine) B (data not shown). TLR mediates the activation of innate immunity and controls the host defense against pathogens.^[54,55] The high level of IFN gamma found in the Reactome Database analysis suggests that the cells grown on poly(carboxybetaine) B reacted as if they were in contact with a virus (as IFN gamma has a highly antiviral effect).^[56] This can be also seen in the KEGG analysis, where another pathway that is typically associated with a viral infection was found to be up-regulated.

In summary, the gene expression study allowed detailed insight into the biological responses of HaCaT cells grown on the polyzwitterionic network A and of cells grown in the presence of network B. While the physical characterization methods only indicated a slightly stronger swellability, and thus a stronger hydration of the poly(carboxybetaine) B, no further differences could be observed in their physical properties, yet the cellular response to the two materials is strikingly different. While there is hardly any difference in the gene expression of HaCaT cells grown on poly(sulfobetaine) A and the GC, the strong hydration of poly(carboxybetaine) B prevents the formation of FA points, which in turn leads to the activation of cell signaling pathways that resemble an inflammatory event or a virus infection, and ultimately drives the non-adhering cells into apoptosis.

3. Conclusion

The interaction of cells with a panel of structurally different polyzwitterions has been studied using human keratinocytes (HaCaT cells) as an example. In particular, the investigated

materials differed in their backbone as well as side-chain hydrophobicity, chemical nature of the anionic and cationic groups, and cross-linking density. The data shows that most polyzwitterions are so hydrophilic that they are overall cell-repellent, in agreement with their general perception as low-fouling materials. Therefore, the effect of most of the structural differences of these polymers (e.g., the BMA content or the cross-linking density) on cell adhesion could not be captured. For the few zwitterionic polymers that were sufficiently cell adhesive, namely the polycarboxybetaine A, the pyridinium-bearing sulfobetaine C, and the amphiphilic sulfobetaine E₄, differences between their interactions with HaCaT cells were studied in more detail using immunofluorescence methods and a gene expression assay. The data showed that FA points were formed by all cells cultivated on cell-adhesive substrates, except for the barely cell-adhesive zwitterionic copolymer E₄, for which no such points could be observed by fluorescence microscopy. Not surprisingly, FAs are needed for cell adhesion and elongation on polyzwitterions. Still, a clear chemical structural feature, or a distinct physical property that would be required for the formation of such FAs could not be identified from the studied sample set, so that further model systems will have to be synthesized in order to clarify this aspect. The genes expressed by the cells grown on the cell-adhesive poly(sulfobetaine) A were not fundamentally different from the genes of the GC. Thus, poly(sulfobetaine) A is a fully biocompatible, yet cell-adhesive polyzwitterion. Furthermore, this assay showed a strong inflammatory response of the cells that were grown in the presence of the non-adhesive poly(carboxybetaine) B, most likely because they cannot adhere to this highly hydrated surface. In any case, this study corroborates that zwitterionic materials can be cell-adhesive in exceptional cases, while the majority are not, and shows that immunofluorescence and gene expression assays help to understand cellular adhesion on polyzwitterionic surfaces in more detail. Further studies should focus on a sample set based on the barely cell-adhesive polyzwitterionic material E₄, but with more incremental changes of properties, so that more distinct structure-property relationships can be derived.

Besides the mere data here reported, this work can also be considered as a blueprint for a workflow comprising a more detailed molecular biological analysis of polymer materials with unusual bioactivity profiles, in addition to the state-of-the-art physical-chemical and biological characterization methods established in the field.

4. Experimental Section

Polymer Synthesis: Polymers A and B were synthesized by ring-opening metathesis polymerization of the underlying zwitterionic unsaturated oxanorbornene imide monomers as described before.^[11] For this, the zwitterionic monomers were dissolved in freshly distilled 2,2,2-trifluoroethanol (TFE). In separate vials, the catalyst was dissolved in freshly distilled dichloromethane (DCM). Adding the catalyst solution to the monomer solution in one shot initiated the polymerization. The reaction was terminated using ethyl vinyl ether. Precipitation of the reaction mixture into diethyl ether yielded the polymers as slightly brown solids.^[11]

The methacryl-based polymers of series C to E were prepared via statistical free radical copolymerization of the zwitterionic respective monomers with small amounts of photo-reactive 2-(4-benzoylphenoxy)-

ethylmethacrylate (BPEMA), and in the case of series E, additionally varying amounts of the hydrophobic comonomer BMA, employing standard procedures (about 30 wt.% of monomers in trifluoroethanol (TFE), 1 mol% of initiator azoisobutyronitrile (AIBN, relative to the monomers), reaction at 60 °C for about 1d, and purification by dialysis in water). The synthesis of polymers D₁ and D₅ is described in detail in ref. [30], of D₂ in ref. [33] of D₃ in ref. [30], of D₄ in ref. [34], and of E₁ to E₃ in ref. [35]. Polymer C was prepared analogously to D₁, and E₄ analogously to E₁, employing the respective zwitterionic methacrylates which were made as described before.^[30,36]

Surface Immobilization: To obtain surface-attached polymer networks, silicon wafers (for ellipsometry, water contact angle measurements), glass coverslips (for cell culture), or gold substrates (for SPR measurements) were used as substrates. These were functionalized with linker molecules (Figure 2) as described in the literature.^[11] For the unsaturated polymers A and B, networks were synthesized using pentaerythritol-tetrakis(3-mercaptopropionate) as an external cross-linker (Figure 2a). A solution of both components was spin-cast onto the substrate and cross-linked by irradiation with UV-light.^[11] The surfaces were then washed with TFE to remove loose polymer chains. All other polymers contained between 1 and 5 mol% of repeat units carrying the internal UV-cross linker benzophenone (BPEMA). They were also spin-coated onto the respective substrates from solution, directly cross-linked by UV-irradiation, and washed with TFE to remove insufficiently crosslinked polymer chains (Figure 2b).^[30,32,33]

Surface Coating and Formation of Surface-Attached Polyzwitterionic Networks: Polymers were coated on 4-(3-triethoxysilyl)propoxybenzophenone (3EPB) functionalized silicon wafers (Si-Mat, Kaufering, Germany) for physical characterization and on round glass coverslips (15 mm diameter; thickness No. 2; ORSatec, Bobingen, Germany) for cell culture using a SPIN150 spin coater (SPS-Europe, Putten, Netherlands) with the following parameters: 3000 rpm, 500 rpm s⁻¹, and 20 s spinning time. For A and B, 30 mg of the polymer were dissolved in 0.25 mL of a solution of pentaerythritol-tetrakis(3-mercaptopropionate) in 2,2,2-trifluoroethanol (TFE, 0.1:5 = V:V). To this solution, 0.8 mL TFE was added. The samples were cross-linked via UV-irradiation (at 254 nm) with an energy dose of 3 J cm⁻². All other polymers were dissolved in TFE with a concentration of 20 mg mL⁻¹. After layer deposition, UV-irradiation at 254 nm with an energy-dose of 0.5 J cm⁻² was used for cross-linking. Afterwards, all networks were extracted in TFE for 30 min to remove polymer chains not connected to the network. For the SPR experiments, gold-coated high-refractive index glass slides were used, onto which the polymers were immobilized as described in ref. [11]. The spin-coating and irradiation parameters were the same as for the other substrate types.

Physical Characterization: The layer thickness of the polymer networks was measured via ellipsometry on an SE 400 adv (SENTECH Instruments GmbH, Berlin, Germany). Average values from three different spots on the sample were calculated. Water-CAs were determined on an OCA20 setup (Dataphysics Instruments GmbH, Filderstadt, Germany). Again, the average value from three different spots on the sample was used. The topography of the surfaces was imaged using a Dimension FastScan from Bruker (Billerica, MA, USA) equipped with commercial ScanAsist Air cantilevers (also from Bruker, length 115 μm, width 25 μm, spring constant 0.4 N m⁻¹; resonance frequency 70 kHz). All AFM images were recorded in ScanAsist Air-mode. Images were analyzed and processed with Nanoscope Analysis 9.1 software. Swellability of the networks was determined via Surface-Plasmon resonance spectroscopy on an RT2005 RES-TEC device in Kretschmann configuration (Res-Tec, Framersheim, Germany). Full reflectivity curves (reflectivity vs. angle of incidence) were measured against nitrogen and water. The layer-thickness was calculated by simulations of the curves based on the Fresnel equations as described previously.^[11] Swellability was calculated by $Q = d_{\text{swollen}}/d_{\text{dry}}$.

Cell Culture: Prior to the cell culture experiments, the coated samples were sterilized by washing them with ethanol, and drying them. HaCaT cells, a spontaneously immortalized human keratinocyte line^[37] were purchased from Cell Line Service (CLS, Eppelheim, Germany) and cultivated according to the manufacturer's instructions in 5% CO₂ at 37 °C in Dulbecco's Modified Eagle's Medium DMEM (CLS, Eppelheim, Germany) containing 4.5g L⁻¹ glucose, 2 mm L-glutamine, and 10% FCS. For all

experiments, 1×10^5 cells were seeded on uncoated and on coated round glass coverslips in 24 well plates and incubated in FCS-free DMEM to allow the cells to settle. After 4 h, 50% of the Medium was replaced with DMEM with double FCS concentration yielding a normal FCS concentration for further cultivation.

Fibronectin Coating: As an additional control, coverslips were coated with $10 \mu\text{g mL}^{-1}$ fibronectin from human Plasma (Sigma-Aldrich Chemie, Schnelldorf) in Hanks' Balanced Salt Solution, HBSS (VWR, Bruchsaal, Germany).

Cell Compatibility: The Alamar Blue assay was performed to test the cell compatibility and analyzed according to the manufacturer's protocol (Bio-Rad AbD Serotec GmbH, Puchheim, Germany). After 24 h the old medium was removed and replaced with 500 mL DMEM + FCS containing 10% Alamar Blue solution. Cells were cultivated in 5% CO_2 at 37 °C for at least 2 h. Supernatant was centrifuged at 300 g for 5 min and the fluorescence intensity was measured (excitation at 540 nm; measurement at 590 nm) using the Micro-Plate reader Infinite F Nano Plus (Tecan, Crailsheim, Germany). After measurement, cells were washed once with Phosphate Buffered Saline w/o Ca^{2+} , Mg^{2+} (PBS, CLS, Eppelheim, Germany), cultivated as described above for additional 24 h and the experiment was repeated. Three coverslips per sample and time-point were analyzed in a minimum of three independent experiments.

For additional evaluation, phase-contrast images were acquired with a Primovert inverse microscope (Zeiss, Oberkochen, Germany). For the Alamar Blue assay, a minimum of three independent experiments were performed using internal triplicates of all samples.

Live-Dead Staining: Cells were washed twice with PBS and stained 1:200 with Syto 16 (Invitrogen Molecular Probes, Eugene, OR, USA) for live cells and 1:1000 with propidium iodide (PI, Sigma-Aldrich GmbH, Steinheim) for dead cells in pre-warmed DMEM with FCS, for 30 min at 37 °C and 5% CO_2 . A dead control was added as stain control. For this, the cells were pre-treated with 0.1 Triton X 100 for 10 min. Cell viability was determined in H_2O immediately afterwards using the Axio Observer Z1 (Zeiss, Oberkochen, Germany).

Immunofluorescence: HaCaT were fixed with 4% paraformaldehyde (PFA) for 10 min and permeabilized with 0.1% Triton X100 in PBS for 10 min. After the cells were blocked with 5% bovine serum albumin (BSA, Sigma-Aldrich Chemie, Taufkirchen, Germany) in PBS for 30 min, HaCaT were stained with the primary antibody phosho-FAK (Tyr397) recombinant rabbit monoclonal Antibody (ThermoFisher scientific, Schwerte, Germany), 1:1000 in 1% BSA in PBS over night at 4 °C. Alexa Fluor 488 goat anti-rabbit IgG (ThermoFisher scientific, Schwerte, Germany) was used for the detection (1:200 in 1% BSA) and actin filaments were stained with Texas red phalloidin (1:40 in 1% BSA) for at least 1 h. The nuclei were labeled with 300 nM 4',6-diamidino-2-phenylindole (DAPI) in PBS for 10 min and finally washed 3 times with PBS. Slides were mounted with Fluoromount-G (Biozol) and Images were obtained using the Axio Observer Z1 (Zeiss, Oberkochen, Germany) fluorescence microscope.

Microscopy Post-Processing and Illustration: Pictures were post-processed with the software zen 2.6 blue edition (Zeiss, Oberkochen, Germany). Microscopy illustrations were performed minimum in duplicates and representative pictures are shown in this work.

RNA Isolation: HaCaT were incubated in triplicates for 24 h on glass coverslips (GC) and on polyzwitterion networks A and B as described above. For sample preparation from the control and from polyzwitterion A, the supernatant was discarded and the coverslips were placed in new 24 well plates. The cells were washed once with PBS, detached with 200 μL pre-warmed TrypLE TM express, and the suspension was filled up with 800 μL DMEM with 10% FCS. For sample preparation from polyzwitterion network B, the supernatant was used to analyze the gene expression, as the cells did not adhere to this sample. 1 mL supernatant was resuspended and collected in a 1.5 mL tube for RNA isolation. RNA isolation was performed using the Monarch Total RNA Miniprep Kit from New England Biolabs (Frankfurt, Germany) according to the manufacturer's instructions, DNase I treatment included. The Qubit RNA HS Assay Kit (Life technologies Corporation, Eugene, Oregon, USA) was used for the detection of the RNA and was measured using the Invitrogen Qubit 3 Fluorometer (Fisher Scientific, Schwerte, Germany). Samples were sent to the Kompetenzzentrum

Fluoreszenz Bioanalytik, (Regensburg, Germany) to finally analyze the RNA using Affymetrix Microarrays.

Visualization and Analysis of Gene Expression Data: Data analysis was performed using basic R functions (Team, R.C. R: A Language and Environment for Statistical Computing. Available online: <http://www.R-project.org/>, accessed on 15 February 2020) and visualized using the R package ggplot2.^[57] Pathway analysis was performed using the Reactome^[49] and KEGG Database.^[51]

Supporting Information

Supporting Information is available from the Wiley Online Library or from the author.

Acknowledgements

Funding by the Federal Ministry of Education and Research (Bundesministerium für Bildung und Forschung, BMBF) through the VIP+ technology transfer grant ANTIBUG, and by Deutsche Forschungsgemeinschaft (DFG, grant LA 611/14) was gratefully acknowledged.

Open Access funding enabled and organized by Projekt DEAL.

Conflict of Interest

The authors declare no conflict of interest.

Data Availability Statement

The data that support the findings of this study are available from the corresponding author upon reasonable request.

Keywords

cell compatibility, focal adhesion, gene expression, immune response, polyzwitterions

Received: June 4, 2022

Revised: September 21, 2022

Published online: October 17, 2022

- [1] L. N. Chen, C. Yan, Z. J. Zheng, *Mater. Today* **2018**, *21*, 38.
- [2] C. K. Pandiyarajan, O. Prucker, B. Zieger, J. Ruehe, *Macromol. Biosci.* **2013**, *13*, 873.
- [3] Y. Iwasaki, E. Tabata, K. Kurita, K. Akiyoshi, *Bioconjugate Chem.* **2005**, *16*, 567.
- [4] C. M. Nickson, P. J. Doherty, R. L. Williams, *J. Biomater. Appl.* **2010**, *24*, 437.
- [5] M. S. Lord, B. G. Cousins, P. J. Doherty, J. M. Whitelock, A. Simmons, R. L. Williams, B. K. Mithorpe, *Biomaterials* **2006**, *27*, 4856.
- [6] S. Paschke, K. Lienkamp, *ACS Appl. Polym. Mater.* **2020**, *2*, 129.
- [7] B. W. Li, P. Jain, J. R. Ma, J. K. Smith, Z. F. Yuan, H. C. Hung, Y. W. He, X. J. Lin, K. Wu, J. Pfaendtner, S. Y. Jiang, *Sci. Adv.* **2019**, *5*, eaaw9562.
- [8] L. C. Zheng, H. S. Sundaram, Z. Y. Wei, C. C. Li, Z. F. Yuan, *React. Funct. Polym.* **2017**, *118*, 51.
- [9] W. Yang, H. Xue, L. R. Carr, J. Wang, S. Y. Jiang, *Biosens. Bioelectron.* **2011**, *26*, 2454.
- [10] Z. Zhang, T. Chao, S. F. Chen, S. Y. Jiang, *Langmuir* **2006**, *22*, 10072.

- [11] M. Kurowska, A. Eickenscheidt, A. Al-Ahmad, K. Lienkamp, *ACS Appl. Bio Mater.* **2018**, *1*, 613.
- [12] M. Kurowska, A. Eickenscheidt, D. L. Guevara-Solarte, V. T. Widyaya, F. Marx, A. Al-Ahmad, K. Lienkamp, *Biomacromolecules* **2017**, *18*, 1373.
- [13] A. Schneider-Chaabane, V. Bleicher, S. Rau, A. Al-Ahmad, K. Lienkamp, *ACS Appl. Mater. Interfaces* **2020**, *12*, 21242.
- [14] A. Laschewsky, *Polymers* **2014**, *6*, 1544.
- [15] A. B. Lowe, C. L. McCormick, *Chem. Rev.* **2002**, *102*, 4177.
- [16] A. Laschewsky, A. Rosenhahn, *Langmuir* **2019**, *35*, 1056.
- [17] M. Ilcikova, J. Tkac, P. Kasak, *Polymers* **2015**, *7*, 2344.
- [18] N. Wang, B. T. Seymour, E. M. Lewoczko, E. W. Kent, M.-L. Chen, J.-H. Wang, B. Zhao, *Polym. Chem.* **2018**, *9*, 5257.
- [19] Y. Iwasaki, K. Ishihara, *Sci. Technol. Adv. Mater.* **2012**, *13*, 064101.
- [20] L. Mi, S. Jiang, *Angew. Chem., Int. Ed. Engl.* **2014**, *53*, 1746.
- [21] M. Elsbahy, A. Li, F. Zhang, D. Sultan, Y. Liu, K. L. Wooley, *J. Controlled Release* **2013**, *172*, 641.
- [22] B. Li, J. Xie, Z. Yuan, P. Jain, X. Lin, K. Wu, S. Jiang, *Angew. Chem., Int. Ed. Engl.* **2018**, *57*, 4527.
- [23] A. A. Khalili, M. R. Ahmad, *Int. J. Mol. Sci.* **2015**, *16*, 18149.
- [24] S. Hong, E. Ergezen, R. Lec, K. A. Barbee, *Biomaterials* **2006**, *27*, 5813.
- [25] A. van der Flier, A. Sonnenberg, *Cell Tissue Res.* **2001**, *305*, 285.
- [26] K. Burridge, M. Chrzanowska-Wodnicka, *Annu. Rev. Cell Dev. Biol.* **1996**, *12*, 463.
- [27] N. O. Deakin, C. E. Turner, *J. Cell Sci.* **2008**, *121*, 2435.
- [28] S. K. Hanks, M. B. Calalb, M. C. Harper, S. K. Patel, *Proc. Natl. Acad. Sci. USA* **1992**, *89*, 8487.
- [29] P. T. Martinez, P. L. Navajas, D. Lietha, *Biomolecules* **2020**, *10*, 179.
- [30] E. Schonemann, A. Laschewsky, E. Wischerhoff, J. Koc, A. Rosenhahn, *Polymers* **2019**, *11*, 1014.
- [31] O. Prucker, T. Brandstetter, J. Ruhe, *Biointerphases* **2017**, *13*, 010801.
- [32] J. Koc, E. Schonemann, A. Amuthalingam, J. Clarke, J. A. Finlay, A. S. Clare, A. Laschewsky, A. Rosenhahn, *Langmuir* **2019**, *35*, 1552.
- [33] J. Koc, E. Schonemann, R. Wanka, N. Aldred, A. S. Clare, H. Gardner, G. W. Swain, K. Hunsucker, A. Laschewsky, A. Rosenhahn, *Biofouling* **2020**, *36*, 646.
- [34] E. Schonemann, J. Koc, J. F. Karthaus, O. Ozcan, D. Schanzenbach, L. Schardt, A. Rosenhahn, A. Laschewsky, *Biomacromolecules* **2021**, *22*, 1494.
- [35] L. Schardt, A. M. Guajardo, J. Koc, J. L. Clarke, J. A. Finlay, A. S. Clare, H. Gardner, G. W. Swain, K. Hunsucker, A. Laschewsky, A. Rosenhahn, *Macromol. Rapid Commun.* **2021**, *43*, 2100589.
- [36] P. Anton, J. Heinze, A. Laschewsky, *Langmuir* **1993**, *9*, 77.
- [37] P. Boukamp, R. T. Petrussevska, D. Breitzkreutz, J. Hornung, A. Markham, N. E. Fusenig, *J. Cell Biol.* **1988**, *106*, 761.
- [38] G. Altankov, V. Thom, T. Groth, K. Jankova, G. Jonsson, M. Ulbricht, *J. Biomed. Mater. Res.* **2000**, *52*, 219.
- [39] H. K. Kleinman, R. J. Klebe, G. R. Martin, *J. Cell Biol.* **1981**, *88*, 473.
- [40] H. K. Kleinman, L. Luckenbilledds, F. W. Cannon, G. C. Sephel, *Anal. Biochem.* **1987**, *166*, 1.
- [41] M. Nishizawa, K. Takoh, T. Matsue, *Langmuir* **2002**, *18*, 3645.
- [42] M. Ahmed, T. Ramos, P. Wieringa, C. van Blitterswijk, J. de Boer, L. Moroni, *Sci. Rep.* **2018**, *8*, 6386.
- [43] C. Ballestrem, N. Erez, J. Kirchner, Z. Kam, A. Bershadsky, B. Geiger, *J. Cell Sci.* **2006**, *119*, 866.
- [44] R. G. Laughlin, *Langmuir* **1991**, *7*, 842.
- [45] Q. Shao, S. Jiang, *J. Phys. Chem. B* **2014**, *118*, 7630.
- [46] R. Jaksik, M. Iwanaszko, J. Rzeszowska-Wolny, M. Kimmel, *Biol. Direct* **2015**, *10*, 46.
- [47] T. Abbas, A. Dutta, *Cell Cycle* **2011**, *10*, 241.
- [48] G. Liu, C. Yang, J. Liu, T. Huang, L. Lin, L. Gu, Z. Li, M. Chen, *Dev. Comp. Immunol.* **2021**, *124*, 104172.
- [49] M. Gillespie, B. Jassal, R. Stephan, M. Milacic, K. Rothfels, A. Senff-Ribeiro, J. Griss, C. Sevilla, L. Matthews, C. Gong, C. Deng, T. Varusai, E. Ragueneau, Y. Haider, B. May, V. Shamovsky, J. Weiser, T. Brunson, N. Sanati, L. Beckman, X. Shao, A. Fabregat, K. Sidiropoulos, J. Murillo, G. Viteri, J. Cook, S. Shorser, G. Bader, E. Demir, C. Sander, et al., *Nucleic Acids Res.* **2022**, *50*, D687.
- [50] M. Kanehisa, *Protein Sci.* **2019**, *28*, 1947.
- [51] M. Kanehisa, S. Goto, *Nucleic Acids Res.* **2000**, *28*, 27.
- [52] B. Pucci, M. Kasten, A. Giordano, *Neoplasia* **2000**, *2*, 291.
- [53] K. Schroder, P. J. Hertzog, T. Ravasi, D. A. Hume, *J. Leukocyte Biol.* **2004**, *75*, 163.
- [54] K. Takeda, S. Akira, *Int. Immunol.* **2005**, *17*, 1.
- [55] W. Zheng, Q. Xu, Y. Zhang, E. Xiaofei, W. Gao, M. Zhang, W. Zhai, R. S. Rajkumar, Z. Liu, *Virology* **2020**, *17*, 192.
- [56] E. F. Wheelock, *Science* **1965**, *149*, 310.
- [57] H. Wickham, *Use R* **2009**, *1*.